Controlled Fabrication of Gold-Coated 3D Ordered Colloidal Crystal Films and Their Application in Surface-Enhanced Raman Spectroscopy

Lehui Lu,[†] Igor Randjelovic,[†] Richard Capek,[†] Nikolai Gaponik,[‡] Jianhui Yang,[§] Hongjie Zhang,[§] and Alexander Eychmüller*,[‡]

Institute of Physical Chemistry, University of Hamburg, Grindelallee 117, D-20146 Hamburg, Germany, Institute of Physical Chemistry and Electrochemistry, Technical University of Dresden, Bergstrasse 66b, D-01062 Dresden, Germany, and Changchun Institute of Applied Chemistry, Chinese Academy of Sciences, 130022 Changchun, China

Received July 7, 2005. Revised Manuscript Received September 19, 2005

We report an alternative procedure to incorporate gold nanoparticles into 3D ordered colloidal crystal film. The size of gold nanoparticles within the films can be controlled from about 10 nm to about 60 nm by simply varying the gold plating time. The application of the as-prepared films in surface-enhanced Raman spectroscopy (SERS) is investigated by using Rhodamine 6G (R6G) as probe molecules. It is found that the resultant gold-coated 3D ordered colloidal crystal films can be used as SERS substrates, exhibiting excellent enhancement ability.

Introduction

Recently, the incorporation of metal nanoparticles into ordered structures has extensively been investigated since such materials may find exciting applications in catalysis[1,2] and photonic crystals,[3,4] as substrates for surface-enhanced Raman spectroscopy (SERS),[5,6] and as chemical and biological sensors.[7] In addition to their unique optical properties, colloidal crystal films have interesting structural properties such as 3D periodicity and large surface areas which make them desirable as template materials. Consequently, a number of strategies have been developed to incorporate metal nanoparticles into 3D ordered colloidal crystal (3DOCC) films.[3−5,7a,8−12] For example, the layer-by-layer (LBL) technique was used by Caruso et al.[9] to assemble gold nanoparticles into a 3DOCC film of functional styrene microspheres. The styrene microspheres were first modified using positively and negatively charged polyelectrolyte multilayers that formed a 3DOCC film. Subsequently, small gold nanoparticles (6 ± 2 nm) were absorbed onto the polyelectrolyte multilayers. The resulting gold-coated films showed interesting optical properties. Recently, Gu et al.[6,7a] reported a dipping method for the fabrication of metal-coated 3DOCC film of silica microspheres. The 3DOCC film was immersed into a mixture of 10-nm gold or silver nanoparticles and supporting polymer followed by lifting the 3DOCC film out of the solution at a constant speed. During the lifting process, simultaneously both nanoparticles and supporting polymer infiltrated the voids within the 3DOCC film. Finally, the resulting film was calcined at 300 °C to remove the polymer and to immobilize the nanoparticles on the surface of the silica spheres. It was found that the as-prepared silver-coated 3DOCC films possess an excellent SERS enhancement ability, and the gold-coated 3DOCC films could be used as refractive index sensors.

Although the LBL technique and the dipping method are very successful in the fabrication of metal-coated 3DOCC films, previous work in this field was mainly devoted to investigating small nanoparticles since it proved difficult to incorporate large nanoparticles into colloidal crystal films that largely limit the design and practical applications of such materials. Until now, it has still been a significant challenge to incorporate metal nanoparticles with desirable size into 3DOCC films in a controllable manner. In this paper, we report a simple alternative procedure, based on the self-assembly of nanoparticles followed by electroless plating, to incorporate larger gold nanoparticles with diameter ranging from about 10 nm to about 60 nm into 3DOCC film. The resulting gold-coated 3DOCC film can be used as SERS substrates, exhibiting excellent enhancement ability. In contrast to previous studies, the proposed strategy has several advantages: (1) both the assembly of the gold nanoparticles and the following gold plating can be performed in a

* To whom correspondence should be addressed. E-mail: alexander.eychmueller@chemie.tu-dresden.de.
[†] University of Hamburg.
[‡] Technical University of Dresden.
[§] Chinese Academy of Sciences.

(1) Wakayama, H.; Setoyama, N.; Fukushima, Y. *Adv. Mater.* **2003**, *15*, 742.
(2) Li, H.; Wang, R.; Hong, Q.; Chen, L.; Zhong, Z.; Koltypin, Y.; Calderon-Moreno, J.; Gedanken, A. *Langmuir* **2004**, *20*, 8352.
(3) Graf, C.; van Blaaderen, A. *Langmuir* **2002**, *18*, 524.
(4) Liang, Z. J.; Susha, A.; Caruso, F. *Chem. Mater.* **2003**, *15*, 3176.
(5) Tessier, P. M.; Velev, O. D.; Kalambur, A. T.; Rabolt, J. F.; Lenhoff, A. M.; Kaler, E. W. *J. Am. Chem. Soc.* **2000**, *122*, 9554.
(6) Kubo, S.; Gu, Z. Z.; Tryk, D. A.; Ohko, Y.; Sato, O.; Fujishima, A. *Langmuir* **2002**, *18*, 5043.
(7) (a) Gu, Z. Z.; Horie, R.; Kubo, S.; Yamada, Y.; Fujishima, A.; Sato, O. *Angew. Chem., Int. Ed.* **2002**, *41*, 1154. (b) Jiang, C. Y.; Markutsya, S.; Pikus, Y.; Tsukruk, V. V. *Nat. Mater.* **2004**, *3*, 721.
(8) Lu, Y.; Xiong, H.; Jiang, X. C.; Xia, Y. N. *J. Am. Chem. Soc.* **2003**, *125*, 12724.
(9) Liang, Z. J.; Susha, A.; Caruso, F. *Adv. Mater.* **2002**, *14*, 1160.
(10) Tessier, P. M.; Velev, O. D.; Kalambur, A. T.; Lenhoff, A. M.; Rabolt, J. F.; Kaler, E. W. *Adv. Mater.* **2001**, *13*, 396.
(11) Jiang, P.; Bertone, J. F.; Colvin, V. L. *Science* **2001**, *291*, 453.
(12) Velev, O. D.; Tessier, P. M.; Lenhoff, A. M.; Kaler, E. W. *Nature* **1999**, *401*, 548.

10.1021/cm051473d CCC: $30.25 © 2005 American Chemical Society
Published on Web 10/20/2005

controllable manner in aqueous solution and have been extensively investigated;[13−15] (2) the entire experimental procedure is easily performed in a standard wet-chemical laboratory at room temperature; (3) the size of the nanoparticles in the 3DOCC film can easily be controlled by simply adjusting the gold plating time and the 3D ordered structure is still retained; and (4) most importantly, this strategy also provides a general route for incorporating other metal nanoparticles into 3DOCC films.

Experimental Section

Preparation of 3-nm Gold Colloid.[16] To 90 mL of $HAuCl_4$ (2.7×10^{-4} M) aqueous solution was added 2 mL of 1% sodium citrate solution under stirring. After 1 min, 1 mL of freshly prepared 0.075% $NaBH_4$ (in 1% sodium citrate solution) was added all at once with vigorous stirring. The stirring was stopped after 5 min and the mixture was kept at about 4 °C until use.

Preparation and Assembly of 3-Aminopropyltrimethoxysilane (APTMS)-Modified Silica Spheres. 270-nm monodisperse silica spheres were synthesized using a modified Stöber method.[17] Briefly, a solution consisting of 80 mL of absolute ethanol, 28 mL of water, and 4 mL of ammonia (28%−30%) was added to a two-necked, 250-mL round-bottomed flask. After 5 min, 10 mL of 0.2 M tetraethyl orthosilicate (TEOS) in absolute ethanol was injected into the above mixture with vigorous stirring. The reaction was allowed to continue for an additional 6 h at room temperature. After that, 100 μL of APTMS was added and the mixed solution was stirred for an additional 12 h. The resultant APTMS-modified silica spheres were cleaned by consecutive centrifuging, decanting, and redispersing in ethanol by sonication (five times). Removal of aggregates and smaller spheres was performed by fractionation, removing the upper and the lower fractions three times. The APTMS-modified silica spheres were assembled onto a silicon wafer or glass substrate that was vertically placed into the slowly evaporating silica spheres dispersion in ethanol for 2 days.[18] Before use, the silicon wafer and the glass substrate were placed in the freshly prepared piranha solution (1:3 30% H_2O_2:H_2SO_4) at 60 °C for 20 min to clean and were then rinsed thoroughly in deionized water and absolute ethanol.

Organization of Gold Nanoparticles into 3DOCC Films and Gold Plating. The dried colloidal template was then immersed into a gold nanoparticle solution of 6-fold diluted concentration with stirring for 10 h. After being rinsed in deionized water and dried in air, the gold-coated 3DOCC films were dipped into 30 mL of a gold plating solution consisting of 0.4 mM hydroxylamine hydrochloride and 0.1% $HAuCl_4$ with stirring for 6, 10, and 14 min, respectively.

Sample Characterization. SEM images were investigated by a Leo 1550 instrument. AFM (Veeco) measurements were performed in the tapping mode. UV−Vis spectra were recorded with a UV−Vis−NIR spectrophotometer (Cary 500, Varian). Structures of the as-prepared samples were characterized by XRD (Philips; X'pert MPD). Raman spectra were taken using a confocal microprobe Raman system (LabRam I from Dilor, France). The microscope attachment is based on an Olympus Bx40 system. An air-cooled

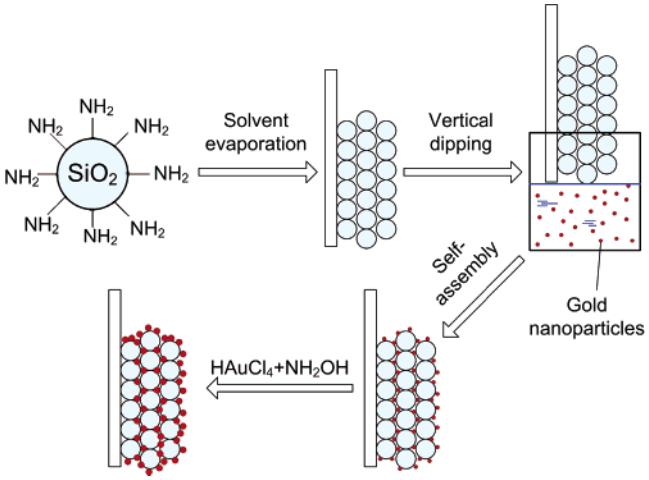

Figure 1. Scheme for the fabrication of metal-coated 3DOCC films.

1024 × 256 pixels CCD (Wright, England) was used as the detector. The excitation wavelength was 632.8 nm from an air-cooled He−Ne laser. The laser light was vertically projected onto the samples.

Results and Discussion

The simple procedure that we have developed for fabricating gold-coated 3DOCC films on flat substrates is shown schematically in Figures 1a−e. In the first step, 3DOCC films were fabricated on a glass substrate or a silicon wafer that was vertically placed in a slowly evaporating ethanol solution of APTMS-modified silica spheres with diameters of 270 nm. After drying in air, the 3DOCC film was immersed in a dilute solution of very small gold nanoparticles (about 3 nm in diameter) for 10 h. During this step, small gold nanoparticles were immobilized on the surface of the APTMS-modified silica spheres via the amine group. Subsequently, the resulting gold-coated 3DOCC film was immersed in a mixture of $NH_2OH/AuCl_4^-$ for gold plating to obtain a gold-coated 3DOCC film with an adjustable size of the gold nanoparticles. To ensure a homogeneous growth of the gold nanoparticles within the 3DOCC films, a 3-nm gold nanoparticle solution with a 6-fold diluted concentration and extensive stirring during the gold plating are necessary. A similar procedure to fabricate the high-quality macroporous metal films was developed earlier by Jiang et al.[19] However, we were forced to apply a number of adjustments to this route in order to gain reproducibility of high-quality films with embedded Au particles.

3DOCC films of APTMS-modified silica spheres of up to several square centimeters are easily prepared by this solvent evaporation method. Figures 2a,b show typical scanning electron microscopy (SEM) images of a 3DOCC film and of a gold-coated 3DOCC film before gold plating. As seen from Figure 2a, the microspheres crystallize in a hexagonal ordered packing with the (111) facet parallel to the silicon wafer substrate. After the incorporation of the gold nanoparticles, the sample clearly retained its original ordering and close packing of the colloidal crystal template, and 3D ordered arrays of the gold-coated silica spheres is revealed from the cleaved edges of the samples. Higher

(13) Menzel, H.; Mowery, M. D.; Cai, M.; Evans, C. E. *Adv. Mater.* **1999**, *11*, 131.
(14) Brown, K. R.; Lyon, A.; Fox, A. P.; Reiss, B. D.; Natan, M. J. *Chem. Mater.* **2000**, *12*, 314.
(15) Charnay, C.; Lee, A.; Man, S. Q.; Moran, C. E.; Radloff, C.; Bradley, R. K.; Halas, N. J. *J. Phys. Chem. B* **2003**, *107*, 7327.
(16) Brown, K. R.; Walter, D. G.; Natan, M. J. *Chem. Mater.* **2000**, *12*, 306.
(17) Stöber, W.; Fink, A.; Bohn, E. *J. Colloid Interface Sci.* **1968**, *26*, 62.
(18) Jiang, P.; Bertone, J. F.; Kwang, K. S.; Colvin, V. L. *Chem. Mater.* **1999**, *11*, 2132.
(19) Jiang, P.; Cizeron, J.; Bertone, J. F.; Colvin, V. L. *J. Am. Chem. Soc.* **1999**, *121*, 7957.

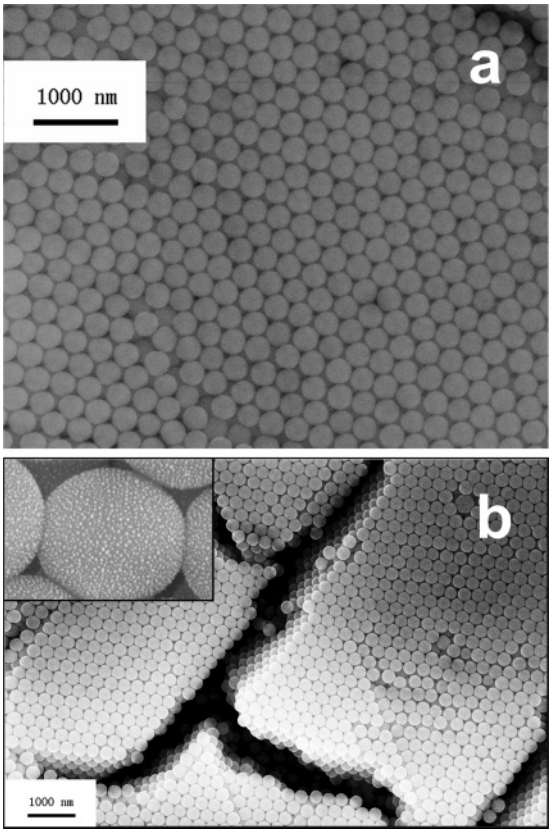

Figure 2. Typical SEM images of (A) a 3DOCC film and (B) a gold-coated 3DOCC film before gold plating with the inset showing a higher magnification image. Scale bar in the inset is 20 nm.

magnification SEM images indicate substantial coverage of gold nanoparticles on the surface of the silica spheres within the 3DOCC film, and the gold nanoparticles are well-separated from each other on the surface (cf. inset in Figure 2b). No obvious nanoparticle aggregation was observed. The prevention of nanoparticle aggregation in the 3DOCC film can be ascribed to the unique structural properties of the 3DOCC film in which the largest voids for the infiltration of the gold nanoparticles are about 45% of the size of the APTMS-modified silica spheres,[20] which are, thus, large compared to the Au nanoparticle size. The coverage of gold nanoparticles on the surface of the silica spheres is evaluated to be approximately 27% from higher magnification SEM images consistent with previously reported coverages of gold nanoparticles on planar amine-functionalized surfaces of solid substrates.[21] The quality of the gold-coated 3DOCC film sensitively depends on the kind of functional molecules and the size and concentration of the gold nanoparticles. Previous research indicated that functionalization of substrate surfaces with different terminal groups has a profound influence on the coverage with gold nanoparticles.[22] Our initial attempt to organize 12-nm gold nanoparticles into a 3DOCC film is less successful most probably because these particles are too large to infiltrate them completely into the whole interstitial

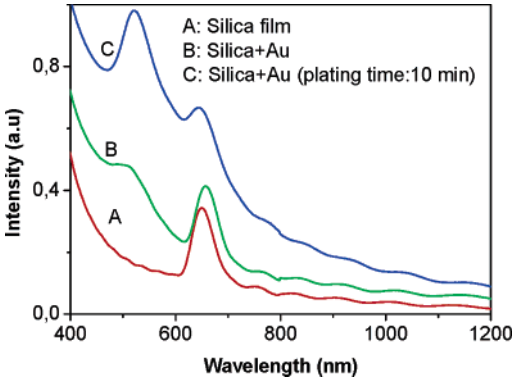

Figure 3. UV−Vis extinction spectra of (A) a 3DOCC film and a gold-coated 3DOCC film (B) before and (C) after gold plating for 10 min.

space of the 3DOCC film, and electrostatic repulsive forces exist between the larger particles which leads to lower coverage of gold nanoparticles being disadvantageous for further gold plating. The dilute gold colloids and proper immersion times are necessary for the formation of high-quality gold-coated 3DOCC films. If these two conditions are properly controlled, aggregation of gold nanoparticles within the 3DOCC film may be avoided. The quality of the initially gold-coated 3DOCC film has a direct effect on the quality of the final materials obtained after gold plating. We rationalize this as follows: during the gold plating, the initial gold nanoparticles attached on the surface of the silica spheres serve as catalysts that accelerate the reduction of the $AuCl_4^-$ ions by hydroxylamine hydrochloride.[23] Therefore, all particle nucleation only occurs on the surface of existing gold nanoparticles, which ensures the growth of the larger gold nanoparticles that are not obtainable by direct methods.[24]

Figures 3a−c show UV−Vis extinction spectra of a 3DOCC film, and a gold-coated 3DOCC film before and after gold plating (10 min). For the plain 3DOCC film a peak at around 650 nm is observed. This peak is attributed to the stop-band of the 3DOCC film which originates from the diffraction of the 3D ordered structures of the colloidal crystal film.[25] Because 3-nm gold nanoparticles are too small to possess a pronounced surface plasmon band at 520 nm that typically characterizes larger gold nanoparticles,[26] the incorporation of the 3-nm gold nanoparticles into the 3DOCC film results in the appearance of only a shoulder near 500 nm, which stems from a suppressed and broadened surface plasmon resonance band as well as from absorption at wavelengths below 520 nm due to d-band to conduction band transitions in gold and scattering from the nanoparticles (Figure 3b).[22,27] When the gold nanoparticles in the 3DOCC film are further immersed in the gold plating solution for 10 min, a strong surface plasmon band appears at about 520 nm besides the peak characteristic of the stop-band of the 3DOCC film. According to Gu et al.,[7a] this spectral char-

(20) Fendler, J. H. *Nanoparticles and Nanostructured Films*; Wiley-VCH: New York, 1998.
(21) Freeman, R. G.; Grabar, K. C.; Allison, K. J.; Bright, R. M.; Davis, J. A.; Guthrie, A. P.; Hommer, M. B.; Jackson, M. A.; Smith, P. C.; Walter, D. G.; Natan, M. J. *Science* **1995**, *267*, 1629.
(22) Westcott, S. L.; Oldenburg, S. J.; Lee, T. R.; Halas, N. J. *Langmuir* **1998**, *14*, 5396.
(23) Brown, K. R.; Natan, M. J. *Langmuir* **1998**, *14*, 726.
(24) Mulvaney, P.; Giersig, M. *J. Chem. Soc., Faraday Trans.* **1996**, *92*, 3137.
(25) Gu, Z. Z.; Meng, Q. B.; Hayami, S.; Sato, O. *J. Appl. Phys.* **2001**, *90*, 2042.
(26) Duff, D. G.; Baiker, A.; Edwards, P. P. *J. Chem. Soc., Chem. Commun.* **1993**, 96.
(27) Kreibig, U.; Vollmer, M. *Optical Properties of Metal Clusters*; Springer-Verlag: New York, 1995.

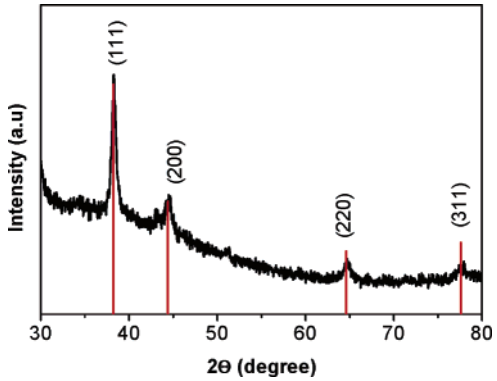

Figure 4. XRD pattern of a gold-coated 3DOCC film after gold plating for 10 min.

acteristic is very important for the application in refractive index sensors. Both surface plasmon band and stop-band depend on the surrounding medium, but their responses to changes in the surrounding medium are not similar since their origin is completely different. The latter is more sensitive to changes in the surrounding medium than the former. For example, the stop-band shifted by 84 nm when the refractive index increased from 1 to 1.538, while the surface plasmon band shifted by 23 nm only. Moreover, as evidenced from Figures 3b,c, the occurrence of the stop-band indicates that the 3D ordered structure of the 3DOCC film was retained after gold plating.

Figure 4 presents a X-ray diffraction (XRD) pattern of the gold-coated 3DOCC film after gold plating (10 min). Four diffraction lines are observed in the XRD pattern at $2\theta \sim 38.2$, 44.5, 64.7, and 77.6°. These diffraction lines are assigned to the (111), (200), (220), and (311) reflections, respectively, for the face-centered cubic structure of metallic Au with the space group $Fm\bar{3}m$ (JCPDS, card no. 04-0784). It is noticed that the ratio between the maximum intensities of the (111) and the (200) diffraction lines is substantially larger than that described in the JCPDS card (4.9 versus 1.9). Similar results are also observed for the ratio between the maximum intensities of the (111) and (220) (or (311)) diffraction lines. These results suggest that in this case the face-centered cubic structure of metallic Au conferred its tendency to nucleate and grow into nanoparticles with their surfaces terminated by the lowest energy (111) facets.[28] Average sizes evaluated from the width of the (111) diffraction peaks using the Scherrer formula (41 nm) coincide well with those from the AFM measurements (43 nm, cf. Figure 5c below).

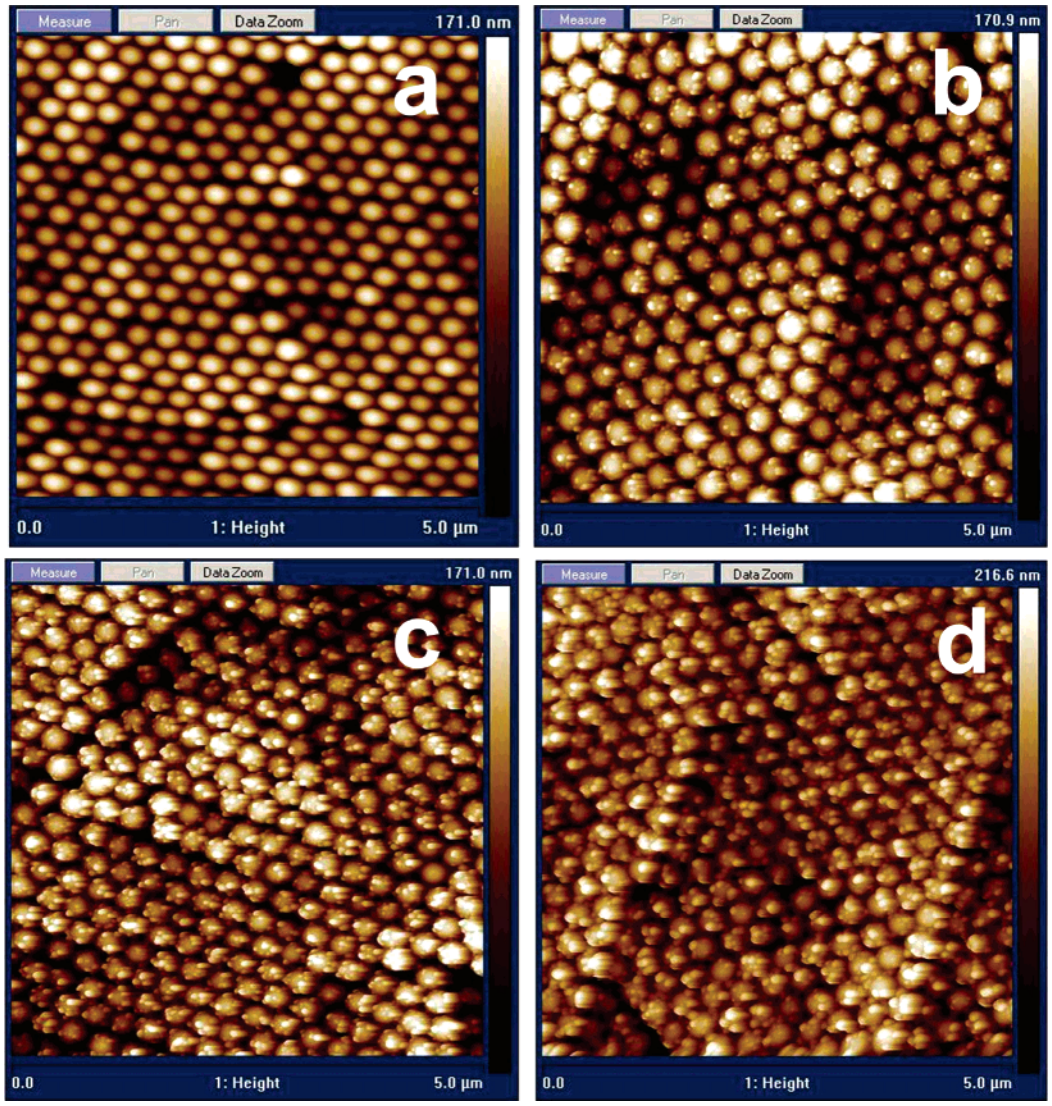

Figure 5. AFM images of (A) a 3DOCC film and a gold-coated 3DOCC film after gold plating for (B) 6 min, (C) 10 min, and (D) 14 min.

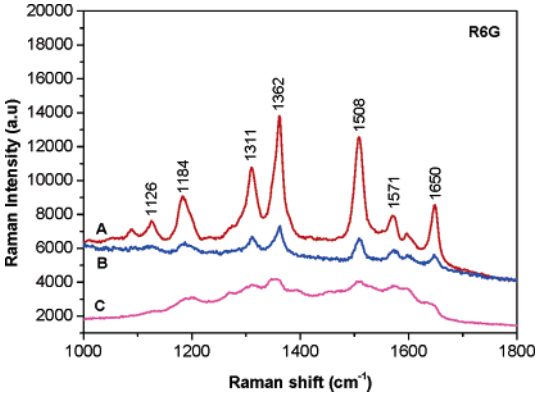

Figure 6. SERS spectra of R6G on different substrates: (A) gold-coated 3DOCC film with 10 min gold plating; (B) gold film prepared according to Natan et al. (cf. ref 14) with 10 min plating; (C) gold film prepared by dipping the substrate directly into the gold plating solution for 10 min. Concentration of R6G: 10^{-7} M; laser wavelength: 632.8 nm.

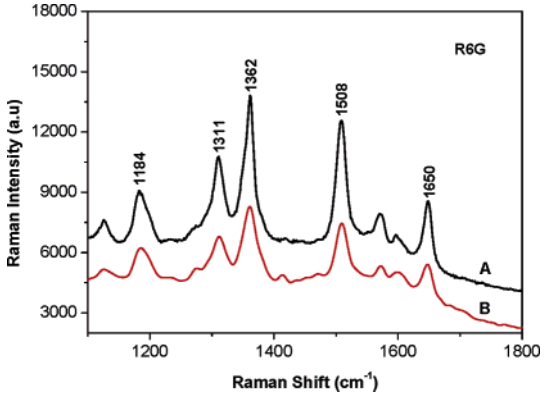

Figure 7. Comparison of SERS intensities between (A) a gold-coated 3DOCC film with 10 min gold plating and (B) a gold-coated 3D disordered silica film with 10 min gold plating. Concentration of R6G: 10^{-7} M; laser wavelength: 632.8 nm.

The gold-coated 3DOCC films are very suitable as SERS substrates since they possess three important characteristics for SERS signal enhancement. First, compared with flat substrates, its 3D ordered macroporous structure increases the accessible surface area for to be detected molecules; second, periodic crevices formed from close-packed spheres are very efficient for SERS signal enhancement;[29] and, third, the nanoparticles attached on the surface of the silica spheres provide a rough surface on the nanometer scale which is very desirable for enhancement of Raman scattering.[27] However, according to previous work,[30] the SERS intensity enhancement depends on the nanoparticles size. Consequently, how to incorporate nanoparticles with desirable sizes into 3DOCC films is of importance for the application of such materials in SERS. Figures 5a−d show atomic force microscopy (AFM) images of a 3DOCC film and a gold-coated 3DOCC film after different gold plating times. The AFM observation of the top surface of the colloidal crystals clearly reveals the hexagonal-type close packing of the silica spheres, consistent with the SEM result. As observed in Figures 5b−d, the original structural properties of the 3DOCC film still remains after plating for 6, 10, and 14 min, respectively, which provide strong evidence of UV−Vis results. The size of the gold nanoparticles on the surface layer of the gold-coated 3DOCC film increases from about 26 nm to about 58 nm with increasing gold plating time and these nanoparticles remain highly dispersed. Thus, in this case it is possible to control the surface roughness defined by the nanoparticle diameter by adjusting the gold plating time. This is of particular importance in the SERS application where the signal enhancement factor is directly related to the nanometer scale roughness.[31]

We evaluated the performance of the as-prepared gold-coated 3DOCC film as SERS substrates using Rhodamine 6G (R6G) as a probe molecule (Figure 6). Sample A is the gold-coated 3DOCC film for 10 min of gold plating. For comparison, we also prepared two kinds of different substrates for SERS applications. One is a gold nanoparticle film prepared according to Natan et al. on a planar glass substrate.[14] Briefly, 3-nm gold nanoparticles were first attached to the APTMS-modified glass, and then the resulting substrate with the 3-nm gold nanoparticle was dipped into the same gold plating solution for 10 min (sample B). The other sample prepared for comparison is made by dipping directly the glass substrate into the same gold plating solution for 10 min (sample C). Subsequently, all samples were dipped into a solution with 10^{-7} M R6G with stirring for 10 min, rinsed with deionized water, and dried with high-purity flowing nitrogen before Raman examination. Figures 6A−C show the SERS spectra for R6G in the Raman shift range between 1000 and 1800 cm^{-1} of those three samples. SERS signals are observed in all cases but sample C gives only a very weak enhancement. As for sample B, the SERS spectrum becomes more intense, but still remains relatively weak. The most intense spectrum is observed with sample A, showing little background noise, and the bands characteristic for R6G can clearly be distinguished in Figure 6A. We also investigated how the periodicity of sample A might change the SERS intensity enhancement. Figure 7 compares the SERS signal intensities of R6G from sample A (Figure 7A) and a disordered gold-coated silica film (Figure 7B). The disordered gold-coated silica film was prepared by the introduction of a small amount of larger APTMS-modified silica spheres (300 nm in diameter) during the assembly of the 270-nm APTMS-modified silica spheres. The other experimental conditions are similar to those of sample A. The SERS intensity of the disordered film was obviously weaker than that of sample A, suggesting that the periodicity of sample A is an important factor for the SERS enhancement. Surprisingly, we found no strong correlation between the SERS intensity enhancement with the increase of the film layer numbers when the layer numbers of the gold-coated 3DOCC film are more than three. Probable reasons for the larger SERS intensity enhancement of sample A are considered as follows: As mentioned above, sample A has two advanced features such as the periodicity and the porous structure. These porous structures can provide larger surface areas that allow more molecules to adsorb.[32] On the other

(28) (a) Yin, Y.; Li, Z.; Zhong, Z.; Gates, B.; Xia, Y.; Venkateswaran, S. *J. Mater. Chem.* **2002**, *12*, 522. (b) Sun, Y.; Xia, Y. *Sience* **2002**, *298*, 2176.
(29) Garcia-Vidal, F. J.; Pendry, J. B. *Phys. Rev. Lett.* **1996**, *77*, 1163.
(30) Krug, J. T.; Wang, G. D.; Emory, S. R.; Nie, S. M. *J. Am. Chem. Soc.* **1999**, *121*, 9208.
(31) Siiman, O.; Bumm, L. A.; Callaghan, R.; Blatchford, C. G.; Kerker, M. *J. Phys. Chem.* **1983**, *87*, 1014.

hand, the periodicity is advantageous for the SERS intensity enhancement.[33,34] First, according to Gaponenko,[34] the photon density of states redistribution may readily occur in a periodic porous metal nanostructure, which results in an increase of the density of optical modes and thus the superior enhancement of the Raman intensity of the detected molecules. Second, the gold-coated silica spheres in sample A can be approximated as larger metal spheres. The diameter (about 270 nm) of these metal spheres is on the order of the laser wavelength (632.8 nm); therefore, the localized plasmon mode can contribute to the SERS intensity enhancement.[29] As shown in Figure 5, the metal spheres in sample A are in contact with others, forming many periodic crevices. The incident light excites plasmons trapped at these crevices, resulting in the formation of a huge electric field in this location. These localized resonant plasmon modes at long-range ordering crevices are able to produce a large SERS enhancement.[29,35] An interesting question to be addressed in future work will be whether the percolation threshold of the metal coating affects the Raman scattering enhancement in our system. Moreover, the SERS performance of the gold-coated 3DOCC film before and after gold plating for 6, 10, and 14 min was also investigated by using the same method. Figure 8A shows the SERS peak intensity of the 1362 cm^{-1} line versus the plating time. No SERS signal is observed for the unplated 3-nm gold-coated 3DOCC film but after 6 min of gold plating the signal increased considerably, maintaining this trend until (at least) 14 min of plating. During the gold plating, the interparticle spacing between the preformed gold nanoparticles on the surface of the silica spheres is further decreased by gold deposition. Such short-range interactions between the gold nanoparticles increases the interparticle coupling, leading to a dramatic enhancement in the SERS activity.[21] Furthermore, the SERS enhancement ability is related to the particle size. For instance, Nie et al. found that 60-nm gold particles showed the most efficient SERS intensity enhancement when the excitation wavelength is about 650 nm.[30] Unfortunately, in our work, it is difficult to incorporate gold nanoparticles with a diameter of more than 60 nm due to the mass-transfer limit, and thus we cannot decide what size is optimal for the SERS enhancement. Figure 8B presents the SERS peak intensity of the 1362 cm^{-1} line as a function of the coverage of the gold nanoparticles on the surface of the silica spheres. The surface coverage was estimated from the magnified AFM images. It is noted that, from 27% to 62% surface coverage, the SERS intensity enhancement increases in a nonlinear fashion. In a previous report,[36] a linear relationship between the SERS intensity and the particle coverage was expected when nanoparticles with similar sizes were assembled into a monolayer on a flat substrate. But in our work, the increase of the surface coverage is due to the growth of the gold nanoparticles.

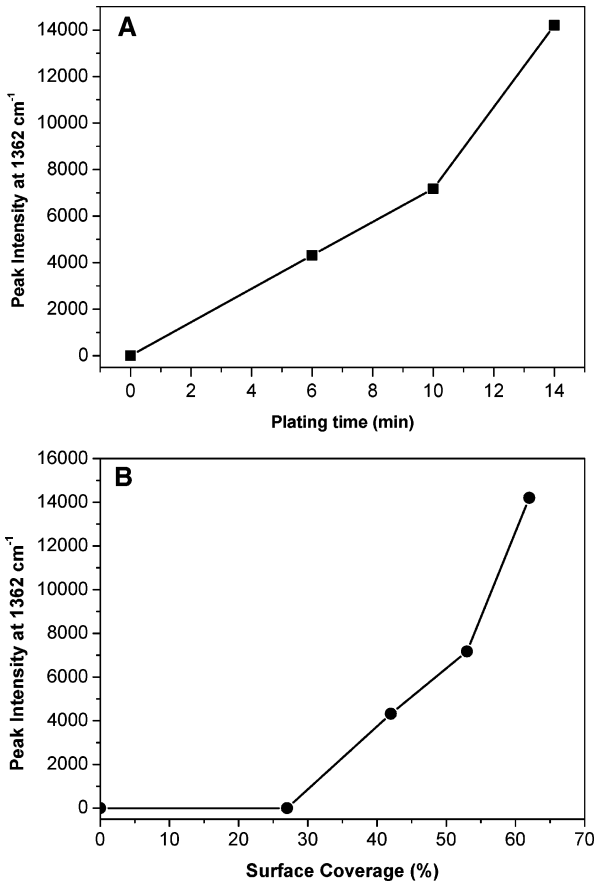

Figure 8. (A) SERS peak intensity of R6G at 1362 cm^{-1} on the gold-coated 3DOCC film versus plating time and (B) plot of the SERS peak intensity of R6G at 1362 cm^{-1} on the gold-coated 3DOCC film as a function of surface coverage.

Therefore, it is reasonable to observe a nonlinear relationship between the SERS intensity enhancement and the surface coverage in this case.

In summary, we have developed a simple and effective procedure for incorporating highly dispersed gold nanoparticles into 3DOCC films with diameter ranging from about 10 nm to about 60 nm in a controlled manner. As-prepared gold-coated 3DOCC films exhibit excellent surface-enhanced Raman scattering (SERS) ability. The periodicity, the long-range ordering porous structure, and the nanoscale roughness are important factors affecting the SERS enhancement activity. Moreover, because the size of the gold nanoparticles can be easily controlled within the 3DOCC films by the present method, the materials with desired particle sizes can be fabricated for other different applications. This procedure can and will be used to incorporate other metal nanoparticles (such as Pt, Pd, and Ag) into 3DOCC films and, thus, it also provides an alternative method for the fabrication of different metal-coated 3DOCC films and their exciting application as sensors and in catalysis.

Acknowledgment. We would like to thank Almut Barck and Andreas Kornowski for XRD and the SEM characterizations and many useful discussions. We also thank the Alexander von Humboldt Foundation and the EU NoE PHOREMOST for financial support.

CM051473D

(32) Kuncicky, D. M.; Christesen, S. D.; Velev, O. D. *Appl. Spectrosc.* **2005**, *59*, 401.
(33) Haynes, C. L.; Van Duyne, R. P.; *J. Phys. Chem. B* **2003**, *107*, 7426.
(34) Gaponenko, S. G. *Phys. Rev. B* **2002**, *65*, 140303R.
(35) Shalaev, V. M. *Nonlinear Optics of Random Media*; Springer: New York, 2000.
(36) Maxwell, D. J.; Emory, S. R.; Nie, S. M. *Chem. Mater.* **2001**, *13*, 1082.